

# Langerhans dendritic cell vaccine bearing mRNA-encoded tumor antigens induces antimyeloma immunity after autotransplant

David J. Chung,<sup>1-4</sup> Sneha Sharma,<sup>1</sup> Madhumitha Rangesa,<sup>1</sup> Susan DeWolf,<sup>5</sup> Yuval Elhanati,<sup>6</sup> Karlo Perica,<sup>7</sup> and James W. Young<sup>1-4,8</sup>

<sup>1</sup>Laboratory of Cellular Immunobiology, Sloan Kettering Institute for Cancer Research, New York, NY; <sup>2</sup>Adult Bone Marrow Transplant Service, Department of Medicine, Memorial Sloan Kettering Cancer Center, New York, NY; <sup>3</sup>Department of Medicine, Weill Cornell Medical College, New York, NY; <sup>4</sup>The Rockefeller University, New York, NY; <sup>5</sup>Leukemia Service, Department of Medicine, <sup>6</sup>Department of Epidemiology and Biostatistics, and <sup>7</sup>Cellular Therapy Service, Department of Medicine, Memorial Sloan Kettering Cancer Center, New York, NY; and <sup>8</sup>Immunology Program, Sloan Kettering Institute for Cancer Research, New York, NY

## Key Points

- Triple antigen-bearing mRNA-electroporated autologous LC vaccines after ASCT for MM are safe and immunogenic.

Posttransplant vaccination targeting residual disease is an immunotherapeutic strategy to improve antigen-specific immune responses and prolong disease-free survival after autologous stem cell transplantation (ASCT) for multiple myeloma (MM). We conducted a phase 1 vaccine trial to determine the safety, toxicity, and immunogenicity of autologous Langerhans-type dendritic cells (LCs) electroporated with CT7, MAGE-A3, and Wilms tumor 1 (WT1) messenger RNA (mRNA), after ASCT for MM. Ten patients received a priming immunization plus 2 boosters at 12, 30, and 90 days, respectively, after ASCT. Vaccines contained  $9 \times 10^6$  mRNA-electroporated LCs. Ten additional patients did not receive LC vaccines but otherwise underwent identical ASCT and supportive care. At 3 months after ASCT, all patients started lenalidomide maintenance therapy. Vaccinated patients developed mild local delayed-type hypersensitivity reactions after booster vaccines, but no toxicities exceeded grade 1. At 1 and 3 months after vaccines, antigen-specific CD4 and CD8 T cells increased secretion of proinflammatory cytokines (interferon- $\gamma$ , interleukin-2, and tumor necrosis factor- $\alpha$ ) above prevaccine levels, and also upregulated the cytotoxicity marker CD107a. CD4 and CD8 T-cell repertoire analysis showed a trend for increased clonal expansion in the vaccine cohort, which was more pronounced in the CD4 compartment. Although not powered to assess clinical efficacy, treatment responses favored the vaccine arm. Triple antigen-bearing mRNA-electroporated autologous LC vaccination initiated at engraftment after ASCT, in conjunction with standard lenalidomide maintenance therapy for MM, is safe and induces antigen-specific immune reactivity. This trial was registered at [www.clinicaltrials.gov](http://www.clinicaltrials.gov) as #NCT01995708.

## Introduction

Multiple myeloma (MM), the second most common hematologic malignancy after non-Hodgkin lymphoma,<sup>1</sup> remains largely incurable despite numerous advances in treatment. High-dose chemotherapy, followed by autologous stem cell transplantation (ASCT) for MM, prolongs progression-free survival (PFS) and overall survival (OS),<sup>2</sup> but disease progression or relapse is inevitable for virtually all patients. The immune system participates in MM disease control,<sup>3-6</sup> and impaired immunity occurs with disease

Submitted 20 August 2021; accepted 3 January 2022; prepublished online on *Blood Advances* First Edition 31 January 2022; final version published online 4 March 2022. DOI 10.1182/bloodadvances.2021005941.

Requests for data sharing may be submitted to David J. Chung ([chungd1@mskcc.org](mailto:chungd1@mskcc.org)).

The full-text version of this article contains a data supplement.

© 2022 by The American Society of Hematology. Licensed under Creative Commons Attribution-NonCommercial-NoDerivatives 4.0 International (CC BY-NC-ND 4.0), permitting only noncommercial, nonderivative use with attribution. All other rights reserved.

evolution,<sup>7-9</sup> thus providing a rationale for immune-based interventions to promote antitumor immunity and to optimize clinical outcomes.

Posttransplant vaccination to control or eliminate residual disease offers an immunotherapeutic strategy to augment responses after ASCT for MM.<sup>10,11</sup> The early posttransplant period consists of a phase of immune reconstitution during which immune-suppressive factors, like regulatory T cells, are decreased in numbers, providing a favorable setting for vaccine-mediated induction of antitumor immunity.<sup>9</sup> Also, the immunostimulatory properties of lenalidomide administered as maintenance therapy after ASCT<sup>12</sup> may enhance vaccine efficacy.<sup>13,14</sup> Therefore, the timing and context of immunization are equally important considerations as the choice of antigen and mode of antigen delivery.

Dendritic cells (DCs) are critical to the onset and modulation of immune responses.<sup>15</sup> Clinical studies have also confirmed the safety and feasibility of DC-based immunization in patients with cancer, albeit with mixed immune and clinical responses.<sup>16</sup> With rare exceptions, past studies have emphasized monocyte-derived DCs, even though CD34<sup>+</sup> hematopoietic progenitor cell (HPC)-derived Langerhans-type dendritic cells (LCs) are more potent stimulators of cytotoxic T lymphocytes (CTLs) against tumor antigens *in vitro*.<sup>17-20</sup> LCs, in contrast to monocyte-derived DCs, can stimulate CTLs *de novo* against a self-differentiation tumor antigen like Wilms tumor 1 (WT1) *in vitro*.<sup>19</sup> Clinical trial data have demonstrated the efficacy of vaccines that include LCs<sup>21</sup> and increased T-cell receptor (TCR) clonality after LC-based vaccination.<sup>22</sup>

Electroporation of DCs with messenger RNA (mRNA) encoding tumor-associated antigens is an effective method for inducing CTLs *in vitro* and *in vivo*.<sup>23,24</sup> Antigen expression after electroporation is more immunogenic than peptide pulsing<sup>23</sup> and eliminates the risk of genome integration associated with retroviral transgenes.<sup>25,26</sup> Electroporation with full-length mRNA also facilitates DCs' processing and presentation of a broader array of peptides tailored to an individual's own class I and II major histocompatibility complex (MHC) to responding T cells and avoids predetermining class I and II MHC restrictions. These attributes of mRNA electroporation also support more robust immune responses than achieved by single class I MHC-peptide pulsing.

Relevant antigen targets for MM beyond B-cell maturation antigen include the cancer/testis antigens CT7 and MAGE-A3 and the self-differentiation antigen WT1. CT7 and MAGE-A3 are the most commonly expressed cancer/testis antigens in MM,<sup>27-29</sup> and their expression is associated with advanced-stage disease<sup>29</sup> and relapse.<sup>30</sup> WT1 expression in the bone marrow of patients with MM also correlates with greater disease burden.<sup>31-33</sup> Finally, antigen-specific immune reactivity against CT7, MAGE-A3, and WT1 has been demonstrated in MM.<sup>32-35</sup>

Many cancer vaccine studies have evaluated single-antigen or restricted epitope targeting. However, simultaneously targeting >1 antigen without restricting to a specific MHC should enhance the extent and breadth of immune responses, leading to improved clinical outcomes. Therefore, we performed a phase 1 clinical study to determine the safety and immunogenicity of vaccination with autologous CD34<sup>+</sup> HPC-derived LCs electroporated with CT7, MAGE-A3, and WT1 mRNA for MM after ASCT. We assessed clinical

outcomes and sequential postvaccination immune responses over time for each participant, as well as between individuals.

## Materials and methods

### Patients and clinical trial design

This clinical trial (#NCT01995708) enrolled patients with symptomatic MM, who were within 12 months of starting induction therapy, had achieved a very good partial response (VGPR) or better by International Myeloma Working Group (IMWG) criteria after induction therapy, had not undergone prior ASCT, and were eligible for ASCT by standard institutional criteria. This phase 1 study tested safety and toxicity and also assessed immune responses stimulated by CT7, MAGE-A3, and WT1 mRNA-electroporated autologous CD34<sup>+</sup> HPC-derived LCs (supplemental Figure 1). The choice of induction therapy was not dictated by the trial. A bone marrow biopsy specimen positive for  $\geq 1$  of the 3 target antigens (CT7, MAGE-A, or WT1) by immunohistochemistry was required. The trial was conducted at Memorial Sloan Kettering Cancer Center (MSKCC), approved by the Institutional Review and Privacy Board of Memorial Hospital/MSKCC and the US Food and Drug Administration (IND 15365), and conducted in accordance with the Declaration of Helsinki and Good Clinical Practice guidelines.

Twenty patients participated in the study, which consisted of 2 cohorts: a vaccine treatment arm and a control arm. Ten patients received post-ASCT vaccines at  $9 \times 10^6$  LCs per dose (combination of  $3 \times 10^6$  CT7 mRNA-electroporated LCs +  $3 \times 10^6$  MAGE-A3 mRNA-electroporated LCs +  $3 \times 10^6$  WT1 mRNA-electroporated LCs). The other 10 patients did not receive any LC vaccines but otherwise underwent identical cytoreduction, ASCT, and standard supportive care. Patients in the vaccine arm received a total of 3 vaccines: a priming immunization on day +12 post-ASCT, followed by boosters on days +30 and +90 post-ASCT. At  $\sim 3$  months after ASCT, all patients started lenalidomide maintenance therapy as per standard of care post-ASCT.

For this trial, the vaccine was considered promising if >5 of the 10 patients in the vaccine arm had an immunologic response. For cytokine secretion and activation epitope expression, a positive T-cell response was defined as a greater than twofold increase over pre-vaccine levels. The decision rule aimed to identify an agent that produced an immunologic response rate >50%. The error rates of missing a promising agent or selecting a nonpromising agent were set at a maximum of 10%. The decision rule and error rates were devised using a historical database of vaccine trials performed at MSKCC.<sup>36</sup> For clonality, a positive T-cell response required an increase above baseline without respect to the degree of increase because there are no validated metrics to provide cutoffs for determining significance.

### Antigen screening

Immunohistochemistry confirmed relevant antigen expression in formalin-fixed paraffin-embedded bone marrow biopsy specimens using monoclonal antibodies specific for CT7/MAGE-C1 (monoclonal antibody CT7-33),<sup>37</sup> MAGE-A3 (M3H67),<sup>27</sup> and WT1 (6F-H2; DAKO).<sup>27,29,37</sup> The degree of staining for each antigen on CD138<sup>+</sup> malignant plasma cells was graded as follows: negative; focal, <5%; +, 5% to 25%; ++, 25% to 50%; +++, 50% to 75%;

and + + + +, >75%. Study eligibility required a positive stain (focal to + + + +) for  $\geq 1$  of the 3 antigens.

### Generation of human LCs for vaccines

Granulocyte colony-stimulating factor–elicited CD34<sup>+</sup> HPCs ( $2 \times 10^6$ /kg actual body weight), collected from patients by leukapheresis at the time of peripheral blood stem cell collection for ASCT, were used to generate enriched LCs in vitro, as reported previously.<sup>17,22</sup> CD34<sup>+</sup> HPCs were cultured in serum-free X-VIVO 15 (Lonza, Basel, Switzerland), supplemented with granulocyte-macrophage colony-stimulating factor, transforming growth factor- $\beta$ , and tumor necrosis factor- $\alpha$  (TNF- $\alpha$ ) over 10 to 12 days in culture. FLT3 ligand and c-kit ligand were also added for the initial 5 to 6 days to enhance CD34<sup>+</sup> progenitor expansion.<sup>17,22</sup> CD34<sup>+</sup> HPC-derived LCs underwent terminal maturation in the presence of inflammatory cytokines TNF- $\alpha$ , interleukin-1 $\beta$  (IL-1 $\beta$ ), interleukin-6 (IL-6), and prostaglandin E<sub>2</sub> for the final 24 to 48 hours.<sup>17,22</sup>

### Production of in vitro–transcribed mRNA

Plasmid expression vectors containing the gene for CT7, MAGE-A3, or WT1 under the control of a T7 (CT7 and MAGE-A3) or SP6 (WT1) promoter were used to synthesize mRNA. Plasmids were propagated in Max Efficiency DH5- $\alpha$  competent cells (Invitrogen) and purified using a Plasmid Maxi Kit (QIAGEN). After linearization, mRNA transcription in vitro was performed with T7/SP6 RNA polymerase (mMESSAGE mMACHINE T7/SP6 Transcription Kit; Ambion). Production of full-length capped mRNA was confirmed by agarose gel electrophoresis, followed by mRNA concentration determination by spectrophotometry.

### Electroporation of LCs

Partially matured LCs were electroporated with CT7, MAGE-A3, or WT1 mRNA on day 12 or 13.<sup>38</sup> LCs were harvested, washed twice, and resuspended in Opti-MEM (Gibco, Invitrogen) to a final concentration of  $15 \times 10^6$  cells per milliliter. Cells (200  $\mu$ L) were mixed with 40  $\mu$ g of mRNA and electroporated in a 2-mm gap cuvette at 700 V for 2 pulses, using a ECM 830 Square Wave Electroporation System (BTX Harvard). After electroporation, cells were returned to culture and terminally matured with inflammatory cytokines for 24 to 48 hours.<sup>17</sup>

### Vaccine administration

After terminal maturation, flow cytometry was used to determine the absolute number of CD83<sup>+</sup>CD86<sup>bright</sup>HLA-DR<sup>bright</sup>CD14<sup>neg</sup> LCs (supplemental Table 1A). Separate pools of mature LCs electroporated with CT7, MAGE-A3, or WT1 mRNA were washed and then combined in equal parts ( $3 \times 10^6$  mRNA-electroporated LCs per antigen based on the number of viable cells) into a single vaccine for intradermal administration at a final dose of  $9 \times 10^6$  mRNA-electroporated LCs per vaccine. The initial priming vaccine used freshly generated LCs, whereas the 2 booster vaccines used viably thawed cells from the initial product, which had been cryopreserved by controlled-rate freezing and stored in liquid nitrogen until the day of administration. After meeting release criteria (supplemental Table 1B), 5 intradermal vaccines ( $10 \times 0.1$  mL) were administered at each of 2 medial limb sites adjacent to axillary or inguofemoral nodes. There were no vaccine production failures, and all patients received the target dose for all 3 vaccines.

### Postvaccination monitoring and clinical outcomes

Erythema and induration at injection sites were measured for delayed-type hypersensitivity reactions 48 hours after each booster vaccine. Adverse events were graded according to Common Terminology Criteria for Adverse Events, version 4.0. Dose-limiting toxicity was defined as grade 3 or higher toxicity. MM disease responses were determined according to IMWG criteria. Multiparameter flow cytometry measured minimal residual disease.<sup>39</sup> Progression-free survival (PFS) and overall survival (OS) were calculated from the time of enrollment and estimated using the Kaplan-Meier method (GraphPad Prism 8.3). The cutoff date for PFS and OS data was 1 June 2021.

### Postvaccination immune response assessments

For patients in the vaccine arm, peripheral blood mononuclear cells (PBMCs) and bone marrow mononuclear cells (BMMCs) were collected prevaccine and then  $\sim 1$  and 3 months after the third and final vaccine. For patients in the control arm, PBMCs and BMMCs were collected at the same time points, with the exception of the BMMC collection at 1 month. Response assessments are described in the following sections.

**Bone marrow immunophenotyping.** BMMCs were incubated with fluorochrome-conjugated antibodies and analyzed on a Cytex Aurora flow cytometer. BUV395-, BUV496-, BUV563-, BUV805-, BV421-, BV510-, BV650-, BV785-, FITC-, SparkBlue-, BB700-, BB790-, PE-, PE-CF594-, PE-Cy7-, A647-, A700-, and APC-Vio770-conjugated mouse anti-human mAbs included anti-CD3, anti-CD4, anti-CD14, anti-CD16, anti-CD25, anti-CD45RO, anti-CD68, anti-PD-1 (all from BD Biosciences), anti-CD45RA, anti-CD57, anti-CD86, anti-CD127, anti-CCR7, anti-FOXP3, anti-HLA-DR, anti-LAG-3 (all from BioLegend), anti-CD8 and anti-CD56 (Miltenyi Biotec), anti-TIM-3 (R&D Systems), and SYTOX Blue/viability (Thermo Fisher). Gates were set for collection and analysis of  $\geq 50,000$  live events. Data analysis, including *t*-distributed stochastic neighbor embedding plot generation, was performed using FlowJo software (FlowJo LLC).

**Antigen-specific T-cell activation and intracellular cytokine secretion.** CD4 and CD8 T-cell specificity for CT7, MAGE-A3, and WT1 was assessed with a restimulation assay.<sup>22</sup> Briefly, PBMCs were cultured with CT7, MAGE-A3, or WT1 mRNA-electroporated autologous LCs generated from the same CD34<sup>+</sup> HPCs used to make patient vaccines. Responder PBMCs were cultured with LCs, at a ratio of 10:1, along with recombinant human IL-2 (10 IU/mL; Chiron, Emeryville, CA) and IL-15 (10 ng/mL; R&D Systems). After 7 days, fresh mRNA-electroporated autologous LCs were added for a second 7-day round of stimulation in the same culture conditions. Cells were then harvested for staining and analysis by flow cytometry, using established methods.<sup>22</sup> T-cell intracellular cytokine levels and activation marker expression were compared for fold changes over prevaccine baseline. Data were analyzed with FlowJo software.

**TCR variable  $\beta$  chain sequencing.** For patients with sufficient cell yields, PBMCs from prevaccination baseline and from 1 and 3 months postvaccines were separated into CD4 and CD8 T-cell fractions using MS columns (Miltenyi Biotec) and cryopreserved for immunosequencing of the CDR3 of T-cell receptor variable  $\beta$

(TCR-V-β) chains using the iRepertoire platform (Huntsville, AL). Extracted genomic DNA was amplified in a bias-controlled multiplex polymerase chain reaction, followed by high-throughput sequencing. Sequences were collapsed and filtered to identify and quantify the abundance of each unique TCR-V-β CDR3.

### Statistics

For immune response assessments, unpaired or paired Student *t* tests assessed differences in expression levels between time points. Statistical analyses were calculated using Prism 8 software (GraphPad), with statistical significance requiring a *P* value < .05. To measure overlap of TCR clones between samples, we calculated the

Morisita similarity index, defined as  $\frac{2 \sum p_i q_i}{\sum p_i^2 + \sum q_i^2}$ , where  $p_i$  and  $q_i$  are the frequencies of clone  $i$  in both samples.

## Results

### Patient characteristics

Thirty-four patients were prescreened for the study (Table 1). Thirty-three (97%) were positive for ≥1 of the 3 required antigens (Table 2). CT7 was the most commonly expressed antigen (85.3%), followed by WT1 (58.8%), and MAGE-A3 (41.2%). The majority of patients (58.9%) expressed >1 antigen, with 26.5% expressing all 3 antigens. There was 1 (2.9%) screening failure with negative expression for all 3 antigens.

Twenty patients enrolled on the trial and were randomized to a vaccine treatment arm (10 patients) or a control arm (10 patients). Table 3 lists the demographics and MM disease characteristics. Median age was 61 years (range, 51-66) for the control arm and 59 years (range, 55-69) for the vaccine arm. All patients received lenalidomide and/or a proteasome inhibitor during induction, with the majority (90%) receiving a triplet regimen. For both arms of the study, 9 patients had achieved a VGPR and 1 patient had achieved a complete response (CR) after induction therapy and preceding ASCT. Of the 13 patients who were eligible but did not proceed on study, 7 deferred upfront ASCT, 3 had progression of disease before ASCT, and 3 did not proceed for reasons unrelated to MM disease status.

### Clinical outcomes

All patients in the vaccine cohort completed the 3 scheduled vaccines, which were tolerated well. Treatment-related adverse events were no greater than grade 1 and self-limited, with the most common being erythema, induration, and mild pruritus at the injection sites, most pronounced after the third vaccine (supplemental Figure 2).

Although not designed to assess clinical efficacy, clinical responses are presented in Table 3 and Figure 1, acknowledging that a higher fraction of patients with Revised International Staging System stage III disease in the control arm and the small sample size limit interpretation. Restaging at 3 months post-ASCT for patients in the control arm found 2 patients with minimal residual disease (MRD)-negative CR, 3 patients with MRD-positive CR, 4 patients with VGPR, and 1 patient with relapsed disease. Restaging at 3 months post-ASCT for patients in the vaccine arm identified 3 patients with MRD-negative CR, 3 patients with MRD-positive CR, and 4 patients with

**Table 1. Antigen expression by CD138<sup>+</sup> bone marrow plasma cells for individual patients**

Patient	CT7	MAGE-A3	WT1
1	+	+	+++
2	Neg	Neg	+
3	++++	++++	+++
4	Focal	Neg	Focal
5	Focal	Neg	+++
6	++	+	Neg
7	Neg	Neg	+
8	++	+	Neg
9	Neg	Neg	Focal
10	+++	++	++
11	++++	Neg	+
12	++	Focal	+
13	Focal	Neg	Neg
14	Focal	Neg	Neg
15	++++	++	++
16	+	++	+++
17	Neg	Neg	+
18	++	+	Neg
19	Focal	Neg	Neg
20	++++	+	Neg
21	Focal	Neg	++
22	+	Neg	Neg
23	Neg	Neg	Neg
24	Focal	Neg	Neg
25	++	Neg	+
26	++	Neg	Neg
27	+	Neg	Neg
28	Focal	Neg	Neg
29	Focal	Focal	+++
30	+	Neg	++
31	+	Focal	Focal
32	++++	+	++
33	+++	+	++
34	++++	++++	Neg

Neg, negative.

VGPR. Restaging at 12 months post-ASCT for patients in the control arm showed 2 patients with MRD-negative CR, 2 patients with MRD-positive CR, 2 patients with VGPR, and 4 patients with relapsed disease. Restaging at 12 months post-ASCT for patients in the vaccine arm showed 5 patients with MRD-negative CR, 3

**Table 2. Antigen expression patterns**

	Antigen expression frequency			Concurrent antigen expression			
	CT7	MAGE-A3	WT1	0	1	2	3
Positive/total	29/34	14/34	20/34	1/34	13/34	11/34	9/34
%	85.3	41.2	58.8	2.9	38.2	32.4	26.5



**Table 3. Patient demographics and disease characteristics**

Patient	Age, y	Sex	MM subtype	R-ISS stage	Induction regimen	Dz status pre-ASCT	Antigen screening			Dz status +3 mo	Dz status +12 mo
							CT7	MAGE-A3	WT1		
<b>Control arm</b>											
4	65	F	IgGλ	III– t(4;14)	RVd	VGPR	Neg	Neg	+1	VGPR	Relapse
6	66	F	IgGκ	II	RVd	VGPR	+3	+2	+2	VGPR	VGPR
8	51	M	IgAλ	III	CyBorD	VGPR	Focal	Neg	Neg	CR (+)	Relapse
10	61	F	IgAκ	I	RVd	VGPR	Neg	Neg	+1	CR (–)	CR (+)
12	65	M	κFLC	II	CyBorD	VGPR	+2	+1	Neg	CR (+)	CR (–)
14	52	F	IgAλ	III– t(14;16)	KRd	CR (–)	Focal	Neg	Neg	Relapse	Relapse
16	56	M	IgGκ	I	KRd	VGPR	+2	Neg	Neg	VGPR	VGPR
17	59	M	IgGκ	II	KRd	VGPR	Focal	Neg	Neg	CR (+)	CR (+)
19	62	F	IgAλ	III– del17	RVd	VGPR	+4	Neg	Neg	CR (+)	CR (–)
20	61	F	IgGκ	II	RVd	VGPR	+4	+4	Neg	VGPR	Relapse
	Median, 61 Range, 51-66	M = 4 F = 6		I = 2 II = 4 III = 4 III = 4		VGPR = 9 CR = 1	8	3	3	VGPR = 4 CR (+) = 3 CR (–) = 2 Relapse = 1	CR (+) = 2 CR (–) = 2 VGPR = 2 Relapse = 4
<b>Vaccine arm</b>											
1	60	M	κFLC	I	Rd	VGPR	Neg	Neg	+1	CR (–)	CR (–)
2	55	F	IgGκ	I	Vd	VGPR	+4	+4	+3	VGPR	Relapse
3	58	M	IgAλ	II	RVd	VGPR	Focal	Neg	+3	CR (–)	CR (–)
5	59	M	IgGκ	I	RVd	VGPR	+2	+1	Neg	CR (–)	CR (–)
7	55	M	κFLC	II– del17	RVd	VGPR	+2	Focal	+1	CR (+)	CR (+)
9	64	M	IgGλ	I	RVd	VGPR	+4	+2	+2	VGPR	CR (–)
11	59	M	IgDλ	III– t(4;14)	RVd	VGPR	Neg	Neg	Focal	CR (+)	CR (+)
13	55	F	IgAκ	II	RVd	VGPR	+1	Neg	Neg	VGPR	CR (–)
15	61	M	κFLC	I	KRd	CR (+)	+2	Neg	+1	CR (+)	CR (+)
18	69	M	IgGλ	II	RVd	VGPR	Focal	Focal	+3	VGPR	VGPR
	Median, 59 Range, 55-69	M = 8 F = 2		I = 5 II = 4 III = 1		VGPR = 9 CR = 1	8	5	8	VGPR = 4 CR (+) = 3 CR (–) = 3	CR (+) = 3 CR (–) = 5 VGPR = 1 Relapse = 1

CyBorD, cyclophosphamide/bortezomib/dexamethasone; Dz, disease; F, female; KRd, carfilzomib (KYPROLIS)/lenalidomide (REVLIMID)/dexamethasone; M, male; Neg, negative; Rd, lenalidomide (REVLIMID)/dexamethasone; R-ISS, Revised International Staging System; RVd, lenalidomide (REVLIMID)/bortezomib (VELCADE)/dexamethasone; Vd, bortezomib (VELCADE)/dexamethasone; (+), MRD positive, (–), MRD negative.

patients with MRD-positive CR, 1 patient with VGPR, and 1 patient with relapsed disease.

For all patients in the study, median follow-up was 59.5 months. For patients in the unvaccinated control arm, 4 remained progression free, with a median PFS of 31 months (range, 3-63). Two patients died, both from MM disease progression, with a median OS of 46 months (range, 12-79). For patients in the vaccine arm, 6 remained progression free, with a median PFS of 54 months (range, 12-85). All patients are alive, with a median OS of 71 months (range, 45-85). There was no clear association between PFS and the extent of CT7, MAGE-A3, or WT1 expression at diagnosis (data not shown).

**Posttreatment immune profiling of the bone marrow microenvironment**

Immunophenotyping of the bone marrow microenvironment after vaccination, compared with prevaccine levels and summarized in Figure 2, showed expansion of CD4 and CD8 effector memory T cells (CCR7<sup>neg</sup>CD45RA<sup>neg</sup>), suppression of CD4 and CD8 naive T

cells (CCR7<sup>+</sup>CD45RO<sup>neg</sup>), and upregulation of T cells expressing the immune checkpoint receptor PD-1. For vaccinated patients, CD4 and CD8 effector memory T cells peaked at 1 month (Figure 2B-C), along with expression of PD-1 (Figure 2B) but not LAG-3 or TIM-3 (data not shown). Control patients showed similar patterns at 3 months (Figure 2B-C); 1-month bone marrow samples were not obtained for this cohort. The relative proportions of natural killer cells, regulatory T cells, exhausted/senescent T cells, and myeloid-derived suppressor cells were similar between the 2 cohorts (data not shown). In aggregate, these findings show an inflammatory effector-skewed environment in the early posttransplant period without substantial phenotypic differences between the vaccine and nonvaccine arms.

**Antigen-specific immune reactivity**

To assess antigen-specific reactivity after vaccination, PBMCs obtained at 1 and 3 months after completion of vaccines were restimulated in vitro with freshly generated autologous LCs electroporated with CT7, MAGE-A3, and WT1 mRNA. Samples collected at

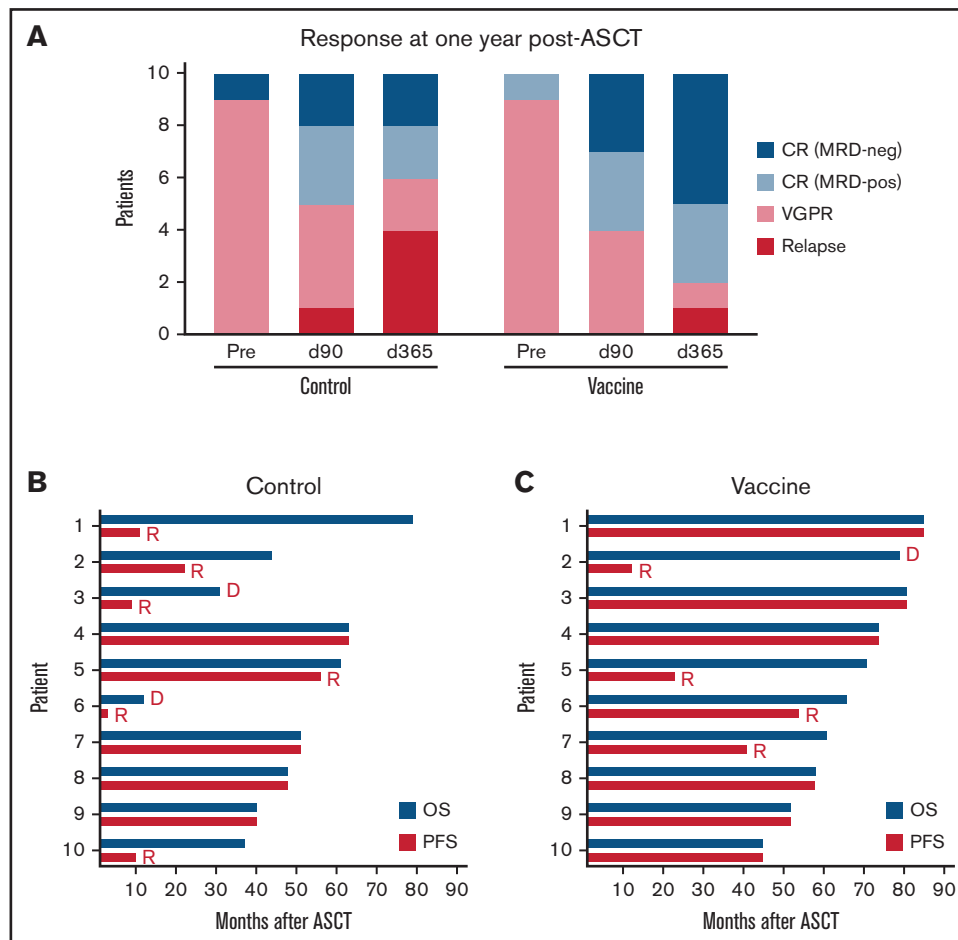


**Figure 1. Clinical responses after ASCT and mRNA-electroporated LC vaccines.** (A) Depth of response pre-ASCT and at days +90 (d90) and +365 (d365) after ASCT. Relapse is also indicated. PFS and OS for patients in the control arm (B) and the vaccine arm (C). D, deceased; R, relapse.

parallel time points from unvaccinated patients served as controls. CD4 T-cell secretion of interferon- $\gamma$  (IFN- $\gamma$ ), IL-2, and TNF- $\alpha$  increased 5.54-, 4.49-, and 3.46-fold, respectively, at 1 month postvaccination, and remained elevated (5.69-, 5.32-, and 2.54-fold, respectively) at 3 months postvaccination (Figure 3A). CD4 T cells also upregulated Mip-1 $\beta$ , a marker of activation, 2.62- and 2.46-fold and CD107a, a marker of degranulation, 2.76- and 4.24-fold, at the 1 and 3-month time points, respectively (Figure 3A). Similar to CD4 T-cell responses, antigen-specific CD8 T-cell secretion of IFN- $\gamma$ , IL-2, and TNF- $\alpha$  increased 5.06-, 4.6-, and 4.68-fold, respectively, at 1 month postvaccination and increased 6.2-, 5.52-, and 2.8-fold, respectively, at 3 months postvaccination (Figure 3B). Upregulation of Mip-1 $\beta$  and CD107a by CD8 T cells was not as pronounced as by CD4 T cells (Figure 3B). Limited cell yields precluded assessment of antigen-specific CTL activity in killing assays. Restimulation assays using BMMCs corroborated the PBMC findings, with increased cytokine secretion and activation marker expression in the CD4 and CD8 T-cell compartments at 3 months postvaccination (Figure 3C-D).

### CD4 and CD8 T-cell clonality after vaccination with mRNA-electroporated LCs

CD4 and CD8 T cells isolated from PBMCs collected after vaccination underwent next-generation deep sequencing of the TCR-V $\beta$

CDR3, with samples from unvaccinated patients providing controls. Pre- to postvaccination TCR repertoire composition varied over time for all patients and was generally similar for the vaccine and control cohorts (Figure 4A), indicating that the post-ASCT TCR repertoire is shaped by factors intrinsic to immune reconstitution after transplant. For both cohorts, the CD4 compartment possessed a higher fraction of low-frequency clones, whereas the CD8 compartment maintained a greater abundance of dominant high-frequency clones (Figure 4A), which has been described in the setting of ASCT for multiple sclerosis.<sup>40</sup> Longitudinal assessment of shared clones from day 12 to day 120 after ASCT, using the Morisita similarity index, revealed consistency between samples over time from the same individuals with infrequent overlap of clones between individuals or between groups (Figure 4B). TCR clonal expansion after ASCT, identified by mean log fold change from baseline at day 12, with emphasis on consistently expanded clones to minimize sample noise, showed increases that were most pronounced in the CD4 compartment of the vaccine cohort (Figure 4C). However, these did not reach statistical significance because of the limited sample size.

### Discussion

Vaccination with triple antigen-bearing mRNA-electroporated autologous LCs initiated at the onset of engraftment after ASCT for MM,

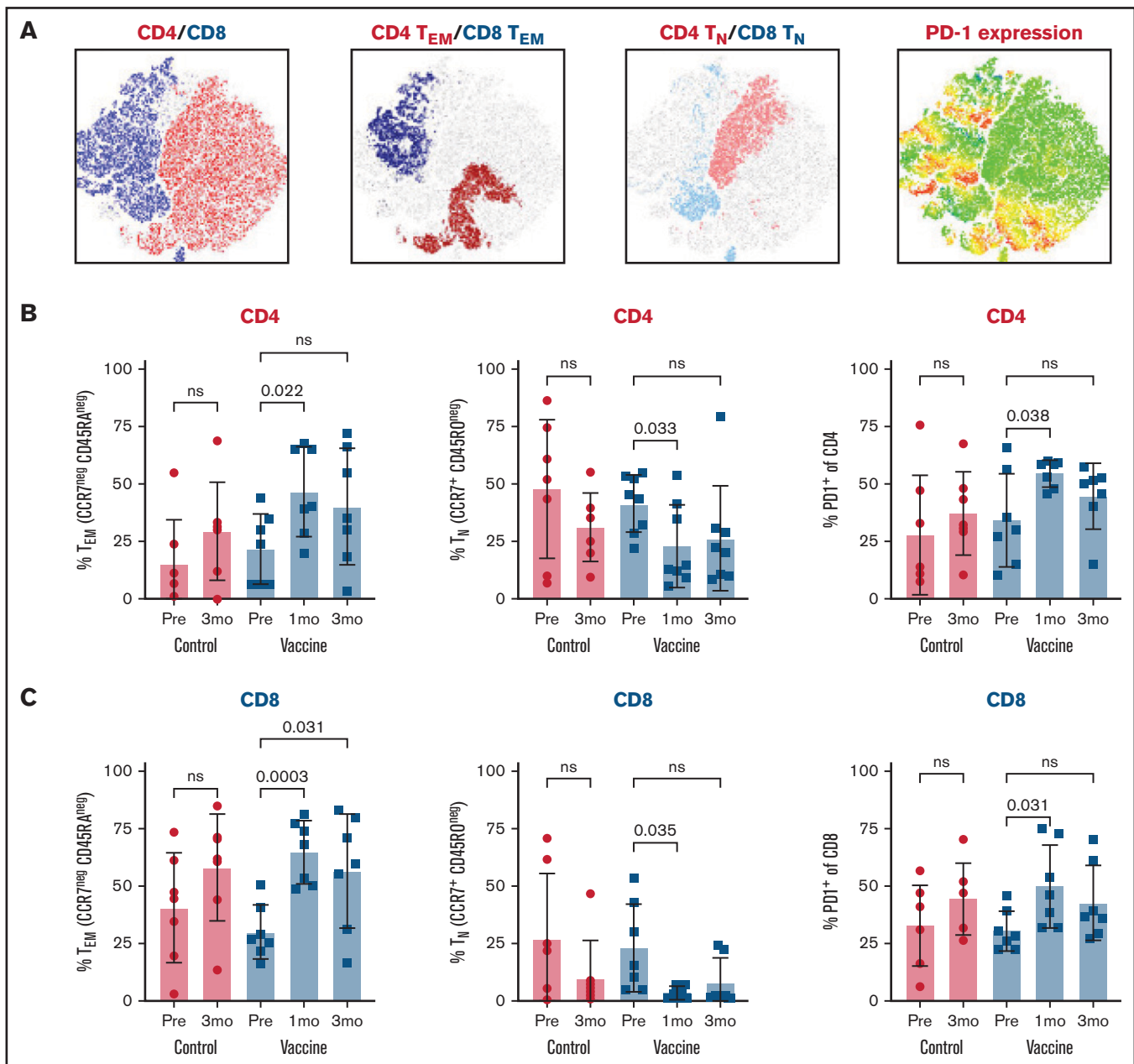


**Figure 2. Bone marrow immunophenotyping after ASCT and mRNA-electroporated LC vaccines.** BMMCs were analyzed by flow cytometry to profile the lymphocyte composition postvaccination in comparison with baseline (prevaccine) and an unvaccinated control cohort. (A) *t*-Distributed stochastic neighbor embedding plots at 3 months after vaccination showing CD4 and CD8 T cells (far left plot), CD4 and CD8 effector memory cells ( $T_{EM}$ ; CCR7<sup>neg</sup>CD45RA<sup>neg</sup>) (middle left plot), CD4 and CD8 naive cells ( $T_N$ ; CCR7<sup>+</sup>CD45RO<sup>neg</sup>) (middle right plot), and PD-1-expressing CD4 and CD8 cells (far right plot). CD4 (B) and CD8 (C) effector memory, naive, and PD-1-expressing cells at 1 and 3 months after vaccines. Pooled data (mean  $\pm$  standard deviation) are shown for patients in the control (red circles) and vaccine (blue squares) arms. ns, not significant; Pre, prevaccine.

followed by lenalidomide maintenance therapy, is safe and feasible. Vaccines are tolerated well, with only mild delayed-type hypersensitivity reactions at injection sites after booster vaccines. Postvaccine immune assessments detected antigen-specific CD4 and CD8 T-cell activation and proinflammatory cytokine secretion, as well as a trend toward greater T-cell clonal expansion. Although not powered to assess clinical efficacy, treatment responses favored the vaccine arm.

The vaccine platform of this study exploited the superior potency of LCs over other DC subtypes,<sup>17-20</sup> combined with electroporation of full-length mRNA<sup>23,24,38</sup> encoding 3 tumor antigens, to promote a broad T-cell response during immune reconstitution in the first 100 days after ASCT.<sup>9</sup> This was coupled with the immune adjuvant activity of posttransplant lenalidomide maintenance therapy.<sup>13,14</sup> Comprehensive immunophenotyping of the bone marrow microenvironment showed generalized activation with increased effector

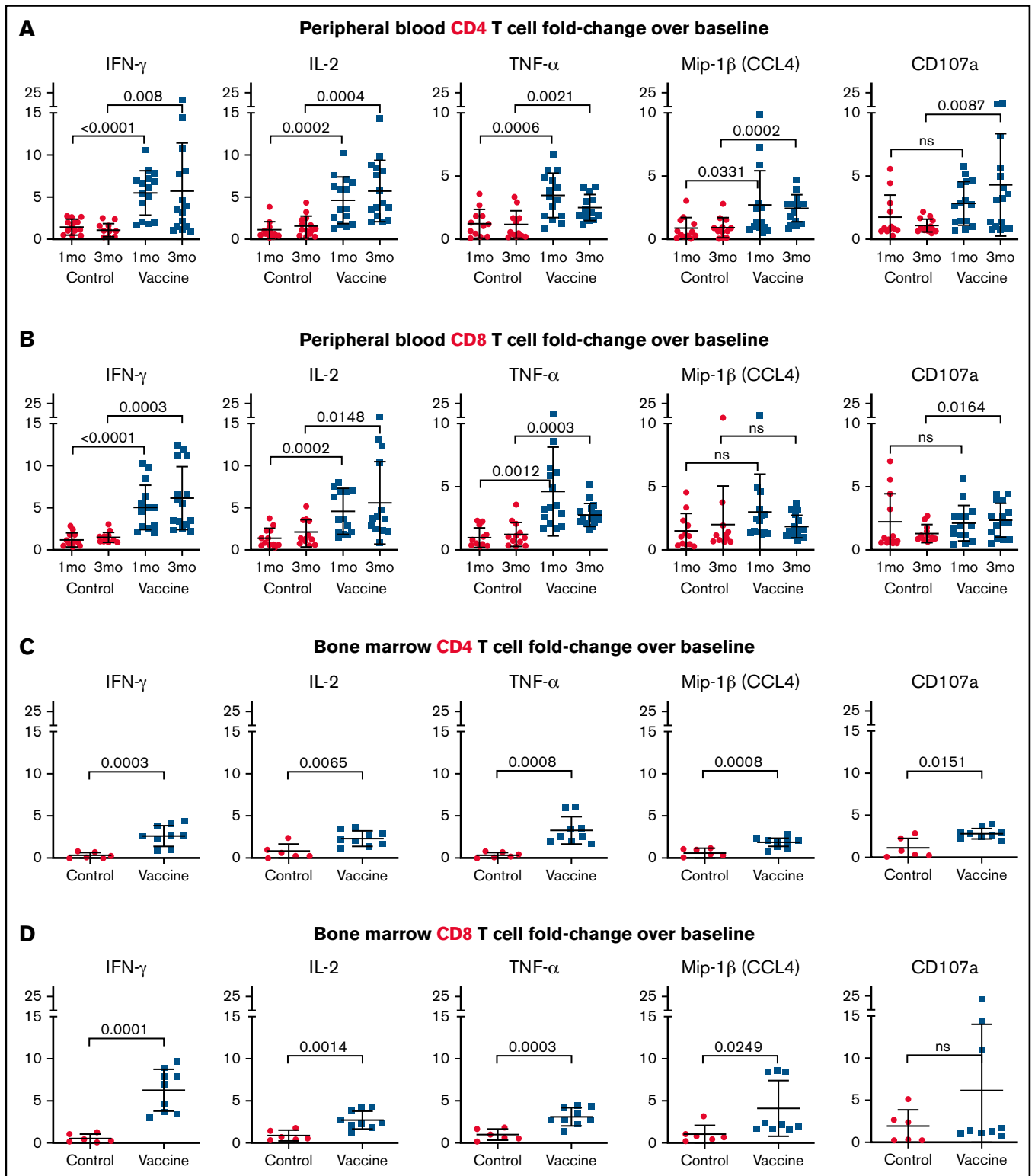


**Figure 3. LC vaccines after ASCT stimulate antigen-specific CD4 and CD8 T-cell cytokine secretion and activation epitope expression.** Postvaccination recall responses to CT7, MAGE-A3, and WT1 mRNA-electroporated LCs were measured as the fold change increase above prevaccine baseline using PBMCs at 1 and 3 months after vaccines (A-B) and BMMCs at 3 months after vaccines (C-D). Fold change in CD4 (A,C) and CD8 (B,D) T-cell proinflammatory cytokine (IFN- $\gamma$ , IL-2, and TNF- $\alpha$ ) secretion and activation epitope (CD107a and Mip-1 $\beta$ ) expression. Pooled data (mean  $\pm$  standard deviation) are shown for patients from the control (red circles) and vaccine (blue squares) arms. ns, not significant.



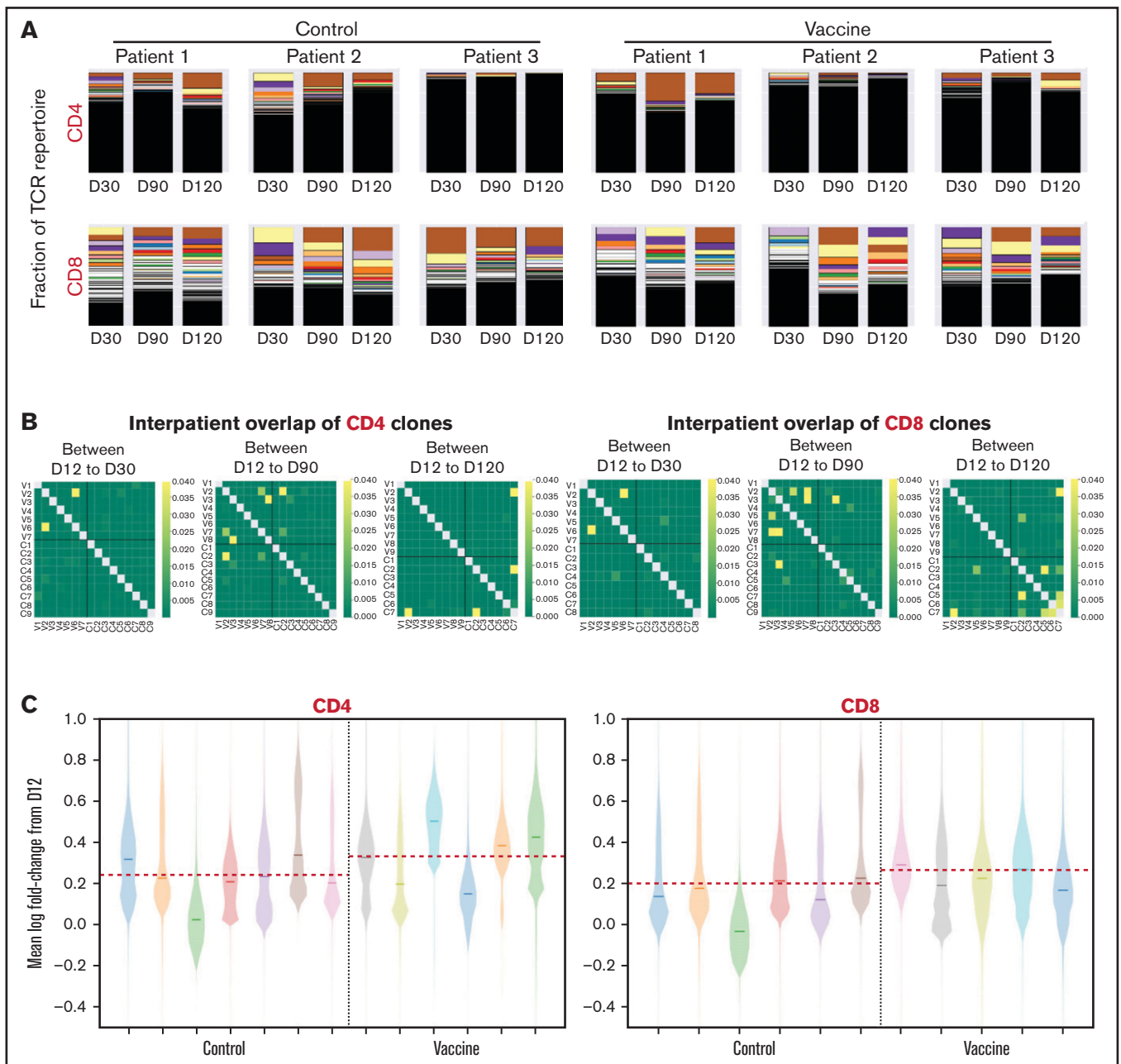


**Figure 4. T-cell clonality after ASCT and vaccination with mRNA-electroporated LCs.** Next-generation deep sequencing of the TCR-V $\beta$  CDR3 was performed on CD4 and CD8 T cells isolated from PBMCs obtained at days 30, 90, and 120 after ASCT and compared with prevaccine levels (day 12). (A) Stacked bar plots of CD4 and CD8 T-cell repertoire composition from 6 representative patients (3 from vaccine arm, 3 from control arm). Each color represents a unique clone, with the higher-percentage clones at the top and lower-percentage clones underneath (low-frequency clones blend together in black). (B) Heat maps of interpatient overlap of CD4 and CD8 T-cell clones calculated using the Morisita similarity index (dark yellow = similar; dark green = dissimilar). V1-V9 along the x- and y-axes represent vaccinated patients. C1-C9 along the x- and y-axes represent control patients. (C) Violin plots representing the mean log fold change in CD4 and CD8 T-cell expansion. Each color represents an individual patient. The red dashed line represents the mean log fold change value in each group. D12, day 12; D30, day 30; D90, day +90; D120, day 120.

memory cell populations in the setting of immune reconstitution post-ASCT. Vaccination-induced antigen-specific activation of CD4 and CD8 T cells was sustained at 3 months after the third and final dose of mRNA-electroporated LCs.

Greater T-cell diversity after immune-based interventions correlates with clinical benefit,<sup>41,42</sup> but altered clonality is an incomplete gauge

of antitumor capacity. This is particularly true of the TCR repertoire after ASCT. Specifically, to our knowledge, this study is the first with TCR analysis in the setting of transplant to include a control cohort demonstrating natural fluctuations in TCR frequency during immune reconstitution after transplant alone. Therefore, this provides a true reference baseline, without which interpretations of changes in the TCR repertoire of the vaccine cohort would have been

skewed much more in favor of a potential vaccine effect. Although there were no significant differences in the overall pattern of T-cell reconstitution or TCR repertoire diversity between the vaccine and control groups in this study, TCR clonotype expansion from the pre-vaccine time point was detected in the CD4 compartment and, to a lesser degree, in the CD8 compartment of vaccinated patients, suggestive of a treatment effect but limited by the small sample size. The nuanced nature of vaccine-mediated changes in the immune repertoire, as well as the challenges of detecting subtle, yet immunologically relevant, changes in TCR clonal composition, highlight the need for higher-resolution assays to map TCRs accurately to their antigen targets and to identify protective TCR clones.

Having generated functionally competent LCs *ex vivo* from patients with MM for this trial, we nevertheless acknowledge the resource limitations for collecting and processing granulocyte colony-stimulating factor–mobilized CD34<sup>+</sup> HPCs as LC precursors, as well as the time, cost, and labor of manufacturing vaccines *in vitro*. These issues restrict the broad clinical application of such LC-based vaccines generated *in vitro*. Studies to circumvent the production process *ex vivo* by activating LCs or other DC subsets directly *in vivo* are ongoing. Despite concerns that the dysfunctional activity of endogenous DCs in MM<sup>43-45</sup> may compromise direct targeting of DCs *in vivo*, DCs from patients with MM can induce MM-specific T cells *ex vivo*.<sup>4,46</sup> Therefore, this implicates factors within the bone marrow tumor microenvironment, like IL-6,<sup>43</sup> that may regulate DC priming of antitumor immunity.

Immune-suppressive cells, including myeloid-derived suppressor cells,<sup>47</sup> regulatory T cells,<sup>48</sup> and tumor-associated macrophages,<sup>49</sup> populate the MM tumor microenvironment. In addition, immune dysfunction, including T-cell exhaustion and/or senescence, correlates with inferior outcomes after ASCT,<sup>9,50,51</sup> characterizes multiply relapsed disease,<sup>52</sup> and is potentially reversible with immune checkpoint blockade.<sup>9,50,52</sup> Therefore, vaccine-extrinsic factors, including elements within the tumor microenvironment and the impaired functional capacity of responding T cells, can subvert optimal T-cell activation,<sup>52</sup> underscoring the complexities of eliciting effective immune responses in the setting of malignancy.

Emerging immune-based therapies for MM include antibody-drug conjugates, bispecific antibody constructs, and chimeric antigen receptor T cells, which have shown promising activity in advanced MM.<sup>53</sup> Durable responses to these treatments are infrequent, but combination strategies with vaccines to prime anti-MM immunity offer an approach to boost responses. For example, vaccination prior to bispecific antibody constructs may augment therapeutic potency by creating pools of antigen-experienced T cells. Vaccines can also promote the expansion and efficacy of chimeric antigen receptor T cells.<sup>54,55</sup>

This study highlights the feasibility of immunizing patients with MM with mRNA-electroporated LCs after ASCT to induce measurable

cellular immune responses against multiple antigens simultaneously. Identification and optimization of rational combinations, timing, and sequencing of DC-based vaccines, including targeting of endogenous DC subtypes, along with other immune-directed interventions, will most likely exert the greatest benefit on improved and durable clinical responses.

## Acknowledgments

The authors thank the patients for participating in the clinical trial. They gratefully acknowledge the contributions of members of the Laboratory of Cellular Immunobiology to the development of this work. They also thank the nurses, advanced practice providers, research staff, and physicians of the Myeloma and Adult Bone Marrow Transplant Services, the Blood Bank Donor Room, and the Cell Therapy Laboratory.

This work was supported by William H. Goodwin and Alice Goodwin and the Commonwealth Foundation for Cancer Research, the Experimental Therapeutics Center of MSKCC (D.J.C.), the Society of Memorial Sloan Kettering (D.J.C.), the Khalily Myeloma Research Fund (D.J.C.), the Guthart Myeloma Research Fund (D.J.C.), the Sawaris Myeloma Research Fund (D.J.C.), American Society of Clinical Oncology Young Investigator Award (S.D.), and Swim Across America, Long Island Sound Chapter. This work was also funded through National Institutes of Health/National Cancer Institute Cancer Center Support Grant P30 CA008748, P01 CA023766, and T32 CA00915.

## Authorship

Contribution: D.J.C. designed and supervised the study, collected data, analyzed and interpreted data, and wrote the manuscript; S.S. and M.R. performed experiments and edited the manuscript; S.D. interpreted data and edited the manuscript; Y.E. analyzed and interpreted data and edited the manuscript; K.P. performed experiments, analyzed and interpreted data, and edited the manuscript; and J.W.Y. designed and supervised the study, interpreted data, and edited the manuscript.

Conflict-of-interest disclosure: The authors declare no competing financial interests.

The content is solely the responsibility of the authors and does not necessarily represent the official views of the National Institutes of Health.

ORCID profiles: D.J.C., 0000-0003-0469-839X; M.R., 0000-0002-5825-2775; S.D.W., 0000-0002-2754-3537; Y.E., 0000-0002-4354-8864; J.W.Y., 0000-0002-0032-6559.

Correspondence: David J. Chung, Memorial Sloan Kettering Cancer Center, 1275 York Ave, New York, NY 10065; e-mail: chungd1@mskcc.org.

## References

1. Siegel RL, Miller KD, Jemal A. Cancer statistics, 2020. *CA Cancer J Clin.* 2020;70(1):7-30.
2. Mikhael J, Ismaila N, Cheung MC, et al. Treatment of multiple myeloma: ASCO and CCO Joint Clinical Practice Guideline [published correction appears in *J Clin Oncol.* 2020;38(21):2469]. *J Clin Oncol.* 2019;37(14):1228-1263.

3. Pellat-Deceunynck C, Jego G, Harousseau JL, Vié H, Bataille R. Isolation of human lymphocyte antigens class I-restricted cytotoxic T lymphocytes against autologous myeloma cells. *Clin Cancer Res*. 1999;5(3):705-709.
4. Dhodapkar MV, Krasovsky J, Olson K. T cells from the tumor microenvironment of patients with progressive myeloma can generate strong, tumor-specific cytolytic responses to autologous, tumor-loaded dendritic cells. *Proc Natl Acad Sci USA*. 2002;99(20):13009-13013.
5. Noonan K, Matsui W, Serafini P, et al. Activated marrow-infiltrating lymphocytes effectively target plasma cells and their clonogenic precursors. *Cancer Res*. 2005;65(5):2026-2034.
6. Goodyear O, Piper K, Khan N, et al. CD8<sup>+</sup> T cells specific for cancer germline gene antigens are found in many patients with multiple myeloma, and their frequency correlates with disease burden. *Blood*. 2005;106(13):4217-4224.
7. Dhodapkar MV, Krasovsky J, Osman K, Geller MD. Vigorous premalignancy-specific effector T cell response in the bone marrow of patients with monoclonal gammopathy. *J Exp Med*. 2003;198(11):1753-1757.
8. Spisek R, Kukreja A, Chen L-C, et al. Frequent and specific immunity to the embryonic stem cell-associated antigen SOX2 in patients with monoclonal gammopathy. *J Exp Med*. 2007;204(4):831-840.
9. Chung DJ, Pronschinske KB, Shyer JA, et al. T-cell exhaustion in multiple myeloma relapse after autotransplant: optimal timing of immunotherapy. *Cancer Immunol Res*. 2016;4(1):61-71.
10. Rosenblatt J, Avivi I, Vasir B, et al. Vaccination with dendritic cell/tumor fusions following autologous stem cell transplant induces immunologic and clinical responses in multiple myeloma patients. *Clin Cancer Res*. 2013;19(13):3640-3648.
11. Cohen AD, Lendvai N, Nataraj S, et al. Autologous lymphocyte infusion supports tumor antigen vaccine-induced immunity in autologous stem cell transplant for multiple myeloma. *Cancer Immunol Res*. 2019;7(4):658-669.
12. McCarthy PL, Holstein SA, Petrucci MT, et al. Lenalidomide maintenance after autologous stem-cell transplantation in newly diagnosed multiple myeloma: a meta-analysis. *J Clin Oncol*. 2017;35(29):3279-3289.
13. Görgün G, Calabrese E, Soydan E, et al. Immunomodulatory effects of lenalidomide and pomalidomide on interaction of tumor and bone marrow accessory cells in multiple myeloma. *Blood*. 2010;116(17):3227-3237.
14. Luptakova K, Rosenblatt J, Glotzbecker B, et al. Lenalidomide enhances anti-myeloma cellular immunity. *Cancer Immunol Immunother*. 2013;62(1):39-49.
15. Cabeza-Cabrerizo M, Cardoso A, Minutti CM, Pereira da Costa M, Reis E Sousa C. Dendritic cells revisited. *Annu Rev Immunol*. 2021;39(1):131-166.
16. Santos PM, Butterfield LH. Dendritic cell-based cancer vaccines. *J Immunol*. 2018;200(2):443-449.
17. Ratzinger G, Baggery J, de Cos MA, et al. Mature human Langerhans cells derived from CD34<sup>+</sup> hematopoietic progenitors stimulate greater cytolytic T lymphocyte activity in the absence of bioactive IL-12p70, by either single peptide presentation or cross-priming, than do dermal-interstitial or monocyte-derived dendritic cells. *J Immunol*. 2004;173(4):2780-2791.
18. Klechevsky E, Morita R, Liu M, et al. Functional specializations of human epidermal Langerhans cells and CD14<sup>+</sup> dermal dendritic cells. *Immunity*. 2008;29(3):497-510.
19. Romano E, Cotari JW, Barreira da Silva R, et al. Human Langerhans cells use an IL-15R- $\alpha$ /IL-15/pSTAT5-dependent mechanism to break T-cell tolerance against the self-differentiation tumor antigen WT1. *Blood*. 2012;119(22):5182-5190.
20. Banchereau J, Thompson-Snipes L, Zurawski S, et al. The differential production of cytokines by human Langerhans cells and dermal CD14<sup>(+)</sup> DCs controls CTL priming. *Blood*. 2012;119(24):5742-5749.
21. Banchereau J, Palucka AK, Dhodapkar M, et al. Immune and clinical responses in patients with metastatic melanoma to CD34<sup>(+)</sup> progenitor-derived dendritic cell vaccine. *Cancer Res*. 2001;61(17):6451-6458.
22. Chung DJ, Carvajal RD, Postow MA, et al. Langerhans-type dendritic cells electroporated with TRP-2 mRNA stimulate cellular immunity against melanoma: results of a phase I vaccine trial. *Oncol Immunology*. 2017;7(1):e1372081.
23. Nair SK, Boczkowski D, Morse M, Cumming RI, Lyerly HK, Gilboa E. Induction of primary carcinoembryonic antigen (CEA)-specific cytotoxic T lymphocytes in vitro using human dendritic cells transfected with RNA. *Nat Biotechnol*. 1998;16(4):364-369.
24. Boczkowski D, Nair SK, Nam JH, Lyerly HK, Gilboa E. Induction of tumor immunity and cytotoxic T lymphocyte responses using dendritic cells transfected with messenger RNA amplified from tumor cells. *Cancer Res*. 2000;60(4):1028-1034.
25. Muul LM, Tuschong LM, Soenen SL, et al. Persistence and expression of the adenosine deaminase gene for 12 years and immune reaction to gene transfer components: long-term results of the first clinical gene therapy trial. *Blood*. 2003;101(7):2563-2569.
26. Hacein-Bey-Abina S, Von Kalle C, Schmidt M, et al. LMO2-associated clonal T cell proliferation in two patients after gene therapy for SCID-X1. *Science*. 2003;302(5644):415-419.
27. Jungbluth AA, Ely S, DiLiberto M, et al. The cancer-testis antigens CT7 (MAGE-C1) and MAGE-A3/6 are commonly expressed in multiple myeloma and correlate with plasma-cell proliferation. *Blood*. 2005;106(1):167-174.
28. Tinguely M, Jenni B, Knights A, et al. MAGE-C1/CT-7 expression in plasma cell myeloma: sub-cellular localization impacts on clinical outcome. *Cancer Sci*. 2008;99(4):720-725.
29. Tyler EM, Jungbluth AA, O'Reilly RJ, Koehne G. WT1-specific T-cell responses in high-risk multiple myeloma patients undergoing allogeneic T cell-depleted hematopoietic stem cell transplantation and donor lymphocyte infusions. *Blood*. 2013;121(2):308-317.
30. Nardiello T, Jungbluth AA, Mei A, et al. MAGE-A inhibits apoptosis in proliferating myeloma cells through repression of Bax and maintenance of survivin. *Clin Cancer Res*. 2011;17(13):4309-4319.

31. Hatta Y, Takeuchi J, Saitoh T, et al. WT1 expression level and clinical factors in multiple myeloma. *J Exp Clin Cancer Res*. 2005;24(4):595-599.
32. Tyler EM, Jungbluth AA, O'Reilly RJ, Koehne G. Wilms' tumor 1 protein-specific T-cell responses in high-risk multiple myeloma patients undergoing T-cell depleted allogeneic hematopoietic stem cell transplantation and donor lymphocyte infusion. *Blood*. 2013;121(2):308-317.
33. Tyler EM, Jungbluth AA, Gnjatich S, O'Reilly RJ, Koehne G. Cancer-testis antigen 7 expression and immune responses following allogeneic stem cell transplantation for multiple myeloma. *Cancer Immunol Res*. 2014;2(6):547-558.
34. Azuma T, Otsuki T, Kuzushima K, Froelich CJ, Fujita S, Yasukawa M. Myeloma cells are highly sensitive to the granule exocytosis pathway mediated by WT1-specific cytotoxic T lymphocytes. *Clin Cancer Res*. 2004;10(21):7402-7412.
35. Tsuboi A, Oka Y, Nakajima H, et al. Wilms tumor gene WT1 peptide-based immunotherapy induced a minimal response in a patient with advanced therapy-resistant multiple myeloma. *Int J Hematol*. 2007;86(5):414-417.
36. Yao TJ, Begg CB, Livingston PO. Optimal sample size for a series of pilot trials of new agents. *Biometrics*. 1996;52(3):992-1001.
37. Jungbluth AA, Chen YT, Busam KJ, et al. CT7 (MAGE-C1) antigen expression in normal and neoplastic tissues. *Int J Cancer*. 2002;99(6):839-845.
38. Chung DJ, Romano E, Pronschinske KB, et al. Langerhans-type and monocyte-derived human dendritic cells have different susceptibilities to mRNA electroporation with distinct effects on maturation and activation: implications for immunogenicity in dendritic cell-based immunotherapy. *J Transl Med*. 2013;11(1):166.
39. Roshal M, Flores-Montero JA, Gao Q, et al. MRD detection in multiple myeloma: comparison between MSKCC 10-color single-tube and EuroFlow 8-color 2-tube methods. *Blood Adv*. 2017;1(12):728-732.
40. Muraro PA, Robins H, Malhotra S, et al. T cell repertoire following autologous stem cell transplantation for multiple sclerosis. *J Clin Invest*. 2014;124(3):1168-1172.
41. Sheikh N, Cham J, Zhang L, et al. Clonotypic diversification of intratumoral T cells following sipuleucel-T treatment in prostate cancer subjects. *Cancer Res*. 2016;76(13):3711-3718.
42. Postow MA, Manuel M, Wong P, et al. Peripheral T cell receptor diversity is associated with clinical outcomes following ipilimumab treatment in metastatic melanoma. *J Immunother Cancer*. 2015;3(1):23.
43. Ratta M, Fagnoni F, Curti A, et al. Dendritic cells are functionally defective in multiple myeloma: the role of interleukin-6. *Blood*. 2002;100(1):230-237.
44. Kukreja A, Hutchinson A, Dhodapkar K, et al. Enhancement of clonogenicity of human multiple myeloma by dendritic cells. *J Exp Med*. 2006;203(8):1859-1865.
45. Leone P, Berardi S, Frassanito MA, et al. Dendritic cells accumulate in the bone marrow of myeloma patients where they protect tumor plasma cells from CD8<sup>+</sup> T-cell killing. *Blood*. 2015;126(12):1443-1451.
46. Racanelli V, Leone P, Frassanito MA, et al. Alterations in the antigen processing-presenting machinery of transformed plasma cells are associated with reduced recognition by CD8<sup>+</sup> T cells and characterize the progression of MGUS to multiple myeloma. *Blood*. 2010;115(6):1185-1193.
47. Görgün GT, Whitehill G, Anderson JL, et al. Tumor-promoting immune-suppressive myeloid-derived suppressor cells in the multiple myeloma microenvironment in humans. *Blood*. 2013;121(15):2975-2987.
48. Braga WM, da Silva BR, de Carvalho AC, et al. FOXP3 and CTLA4 overexpression in multiple myeloma bone marrow as a sign of accumulation of CD4(+) T regulatory cells. *Cancer Immunol Immunother*. 2014;63(11):1189-1197.
49. Asimakopoulos F, Kim J, Denu RA, et al. Macrophages in multiple myeloma: emerging concepts and therapeutic implications. *Leuk Lymphoma*. 2013;54(10):2112-2121.
50. Minnie SA, Kuns RD, Gartlan KH, et al. Myeloma escape after stem cell transplantation is a consequence of T-cell exhaustion and is prevented by TIGIT blockade [published correction appears in *Blood*. 2019;134(21):1878]. *Blood*. 2018;132(16):1675-1688.
51. Parmar H, Gertz M, Anderson EI, Kumar S, Kourelis TV. Microenvironment immune reconstitution patterns correlate with outcomes after autologous transplant in multiple myeloma. *Blood Adv*. 2021;5(7):1797-1804.
52. Visram A, Kourelis T, Dasari S, Anderson E, Kumar SK. Describing the cellular and humoral immune tumor microenvironment and malignant transcriptome across the multiple myeloma disease spectrum. *Blood*. 2020;136(suppl 1):39-40.
53. Shah N, Chari A, Scott E, Mezzi K, Usmani SZ. B-cell maturation antigen (BCMA) in multiple myeloma: rationale for targeting and current therapeutic approaches. *Leukemia*. 2020;34(4):985-1005.
54. Akahori Y, Wang L, Yoneyama M, et al. Antitumor activity of CAR-T cells targeting the intracellular oncoprotein WT1 can be enhanced by vaccination. *Blood*. 2018;132(11):1134-1145.
55. Reinhard K, Rengstl B, Oehm P, et al. An RNA vaccine drives expansion and efficacy of claudin-CAR-T cells against solid tumors. *Science*. 2020;367(6476):446-453.